



Surface and volume photoeffect from metal nanoparticles with electron mass discontinuityIgor E. Protsenko * and Alexander V. Uskov *P. N. Lebedev Physical Institute, Leninsky prospect 53, Moscow 119991, Russia*

Nikolay V. Nikonorov

ITMO University, Kronverksky prospect 49, Saint Petersburg 197101, Russia

(Received 28 March 2021; revised 28 May 2021; accepted 28 May 2021; published 28 June 2021)

Internal quantum efficiencies of the surface photoemission (SPE) and the volume photoemission (VPE) from metal nanoparticles into a semiconductor environment are found and compared with each other, taking into account the discontinuity in the electron effective mass on the metal-semiconductor interface. It is found that SPE is less sensitive to the discontinuity of the electron effective mass than VPE. This advantage, along with other advantages, makes SPE more efficient than VPE for generation of hot electrons from small metal nanoparticles. General formulas for quantum efficiencies and analytical expressions for quantum efficiency on the red photoeffect limit are presented. High efficiency of SPE from spherical gold nanoparticles with the step potential barrier on the metal-semiconductor interface is demonstrated.

DOI: [10.1103/PhysRevB.103.235432](https://doi.org/10.1103/PhysRevB.103.235432)**I. INTRODUCTION**

Photoemission from metal nanoparticles generates “hot” electrons [1,2]. Hot electrons have various applications, for example, in photodetection [3–5] and photocatalysis [6,7]. When metal nanoparticles are incorporated into a semiconductor, the work function of a metal decreases, making hot electron generation possible at the absorption of visible or near IR light of plasmon resonance frequencies, when the electric field inside nanoparticles is high. However, the effective mass of an electron changes when an electron passes the barrier on the metal-semiconductor interface and comes to a semiconductor. In order to satisfy the momentum conservation law, kinetic energy of the electron must exceed the barrier height substantially. Thus the discontinuity in the electron effective mass strongly reduces the photoemission from the volume of a nanoparticle [8,9].

It is well known that the change of the electron effective mass affects the volume photoemission (VPE) as, for example, at the electron beam emittance from metal photoanodes to vacuum [10]. The effective mass variation is important for calculation of parameters of VPE in various systems, for example, for transverse energy spread of electron beams through the rough surface of photocathodes [11], and for two- and three-dimensional electron emission out of a multilayer cathode [12]. The electron effective mass change affects also the electron field and the electron thermionic emissions [13–15].

In contrast, the influence of electron effective mass variation (or the electron effective mass discontinuity) on the metal-environment interface in the case of the surface photoemission (SPE) is less studied than in the case of VPE, in particular, for metal nanoparticles, where SPE is especially

important at certain conditions [16]. SPE from nanoparticles into a semiconductor [17] may be more efficient than VPE [9], even with discontinuity in the electron effective mass [17], which has been confirmed by experiments [7,18].

The purpose of our paper is to prove theoretically that SPE can be more efficient than VPE from metal nanoparticles into a semiconductor, because SPE is less reduced by the change of the electron effective mass than VPE. Such an advantage of SPE must be taken into account and will help, in the future, to reach the maximum efficiency of generation of hot photoelectrons.

Absorption of an electromagnetic field in collisions of electrons with the metal-environment interface (surface) followed by SPE has been studied for a long time [19] (see also [17] and references therein). It is well known that SPE is sensitive to discontinuities in the potential barrier, dielectric function, and electron effective mass on the metal-environment interface [20,21]. The general approach for SPE in metal nanoparticles [16], developed with quantum theory of perturbations in the continuous spectrum [20,21], takes into account all such discontinuities.

The procedure of [20,21] is similar to the approach with incoming wave solutions [22,23] or so-called inverse low-energy electron diffraction (iLEED) states [24]. We derive an expression for the photoemission probability amplitude in Appendix A and show there the relation of our procedure and the approach with iLEED states.

The approach [16] has been used, in particular, for studies of electron photoemission from plasmonic nanoantennas [25], comparison between the surface and the volume photoemission from plasmonic nanoparticles [17], broadening of plasmonic resonance due to electron collisions with the nanoparticle boundary [26], and enhanced electron photoemission by collective resonances in nanoparticle lattices [27].

*protsenk@gmail.com

This has been done, so far, without taking into account the electron mass discontinuity.

In this paper we extend the study of [16,17] and compare SPE and VPE taking into account the discontinuity in the electron effective mass along with other discontinuities on the interface of metal nanoparticles and a semiconductor environment.

In Secs. II and III we present general formulas for internal quantum efficiencies η_{SPE} of SPE and η_{VPE} of VPE valid for an arbitrary barrier on the interface in the “flat” interface approximation [20,21]. In Sec. IV we consider and compare SPE and VPE using the example of the step potential barrier on the metal-semiconductor interface and demonstrate how the discontinuity in the electron effective mass affects the photoeffect. We find explicit expressions for η_{SPE} and η_{VPE} near the red limit of the photoeffect, and demonstrate that $\eta_{\text{SPE}} > \eta_{\text{VPE}}$, which means that SPE is more efficient than VPE. We will see that $\eta_{\text{SPE}} > \eta_{\text{VPE}}$ also when the localized plasmon resonance in the nanoparticle is excited. We illustrate the results by examples of the photoemission from gold spherical nanoparticles in different semiconductor environments. In the discussion section we explain physical reasons why SPE is less affected by the change in the electron effective mass than VPE. Results are summarized in the conclusion. Derivation of formulas of the main text are presented in Appendices A–C.

II. SURFACE PHOTOEMISSION

Quantitative characteristics of SPE and VPE in nanoparticles, convenient for comparison, are their *internal quantum efficiencies* $\eta_{\text{SPE,VPE}}$. Internal quantum efficiency is the ratio of the number of photoelectrons generated per second to the number of photons absorbed per second in the nanoparticle:

$$\eta_{\text{SPE,VPE}} = \frac{J_{\text{SPE,VPE}}}{R_{\text{abs}}}, \quad R_{\text{abs}} = \int_{V_p} r_{\text{abs}} dV, \quad r_{\text{abs}} = \frac{\varepsilon''_{\text{in}} |\mathcal{E}_{\text{in}}|^2}{2\pi\hbar}. \quad (1)$$

Here $J_{\text{SPE,VPE}}$ is a surface or a volume photoemission current from a nanoparticle, expressed in the number of photoelectrons per second; R_{abs} is the number of photons absorbed in the volume V_p of the nanoparticle per second; r_{abs} is the photoabsorption rate in the unit of volume; \mathcal{E}_{in} is the amplitude of the electric field inside the nanoparticle; $\varepsilon''_{\text{in}}$ is the imaginary part of the dielectric function of the metal. In general, $\varepsilon''_{\text{in}}$ takes into account Landau damping [26].

According to [16], SPE current is

$$J_{\text{SPE}} = \int_{k_z, k_{\parallel}} dj_{\text{SPE}} \int_{S_p} |\mathcal{E}_{\text{in}}^{(n)}|^2 dS_p, \quad (2)$$

where $\mathcal{E}_{\text{in}}^{(n)}$ is the component of the electric field inside the nanoparticle near its surface and normal to this surface of the area S_p . Differential surface density dj_{SPE} of the photocurrent per unit of $|\mathcal{E}_{\text{in}}^{(n)}|^2$ is

$$dj_{\text{SPE}} = (\hbar\tilde{k}_{1z}/m_{\text{out}})|c_+|^2 dn_s. \quad (3)$$

Notations of parameters in Eq. (3) are explained below.

The first integration by dj_{SPE} in Eq. (2) is by electrons in their initial states before absorption. The number dn_s of such

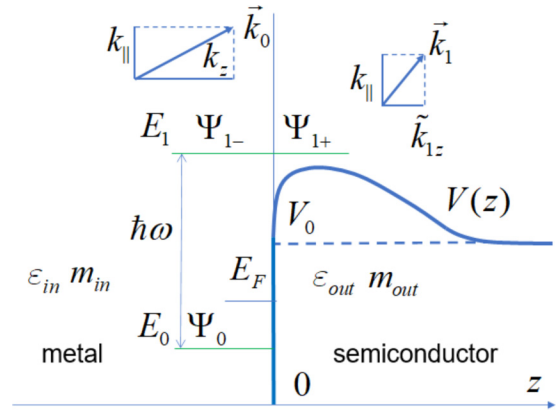


FIG. 1. Scheme of the metal-semiconductor interface. E_0 (E_1) are energies of initial (final) states of an electron before (after) absorption of photon $\hbar\omega$; V_0 is the energy of the bottom of the conduction band of the semiconductor environment; $V(z)$ is the Schottky barrier. Definitions of other parameters are given in the text.

electrons with wave numbers in a small interval from k_0 to $k_0 + dk_0$ is

$$dn_s = f_F(k_0^2) [1 - f_F(k_0^2 + k_\omega^2)] k_{\parallel} dk_{\parallel} dk_z / 2\pi^2.$$

Here $k_\omega^2 = k_z^2 + k_{\parallel}^2$; k_z (k_{\parallel}) is the component of the wave vector of the electron perpendicular (parallel) to the interface, $k_\omega^2 = 2m_{\text{in}}\omega/\hbar$,

$$f_F(y) = \{1 + \exp[(\hbar^2 y / 2m_{\text{in}} - E_F) / K_B T]\}^{-1}$$

is the Fermi distribution function, m_{in} is the effective mass of an electron inside the nanoparticle, K_B is the Boltzmann constant, and E_F is Fermi energy.

The potential barrier on the metal-semiconductor interface and some parameters used throughout the paper are shown in Fig. 1. The integration by dj_{SPE} in Eq. (2) includes integrations by components k_z and k_{\parallel} of wave vectors of electrons.

The wave-vector component k_{\parallel} is preserved at the photoemission because of the momentum conservation law; m_{out} and \tilde{k}_{1z} are the effective electron mass and the component of the electron wave vector normal to the interface outside the nanoparticle far from the interface:

$$\tilde{k}_{1z} = \sqrt{[k_z^2 + k_\omega^2 - k_V^2 - k_{\parallel}^2 (r_m - 1)] / r_m}, \quad (4)$$

where $k_V = \sqrt{2m_{\text{in}}V_0}/\hbar$ and $r_m = m_{\text{in}}/m_{\text{out}}$. We suppose that $r_m > 1$. The photoelectron with real \tilde{k}_{1z} has enough energy to pass the barrier and move away the nanoparticle. Imaginary \tilde{k}_{1z} means that the electron has low energy, it cannot pass through the barrier and remains in the nanoparticle.

Following [16] we express the probability amplitude of SPE of a single electron as $c_+ \mathcal{E}_{\text{in}}^{(n)}$, where

$$c_+ = c_+^{(0)} - \frac{|e|\varepsilon_{\text{in}}}{W(\hbar\omega)^2 \varepsilon_{\text{out}}} \int_{+0}^{\infty} V' \Psi_0 \Psi_{1-} dz, \quad W = \Psi_{1-} \Psi'_{1+} - \Psi_{1+} \Psi'_{1-}, \quad (5)$$

and the prime means the differentiation with respect to z . The first term in Eq. (5) is

$$c_+^{(0)} = \frac{|e|m}{(\hbar\omega)^2 m_{\text{in}} W} \left\{ \left[(r_\varepsilon r_m - 1) \left(E_0 + \frac{\hbar\omega}{2} \right) - r_\varepsilon r_m V_0 \right] \times \Psi_0 \Psi_{1-} + (r_\varepsilon - 1) m_{\text{in}} \hbar^2 \Psi_0' \Psi_{1-}' / 2m^2 \right\} \Big|_{z=0}, \quad (6)$$

which describes discontinuities of parameters in $z = 0$. The second term in Eq. (5) depends on the potential barrier $V(z)$ in the semiconductor environment. $V(z)$ is changed in the z direction perpendicular to the interface and assumed constant (flat) parallel to the interface [20,21]; e is electron charge, $r_\varepsilon = \varepsilon_{\text{in}}/\varepsilon_{\text{out}}$, ε_{in} (ε_{out}) is a dielectric function inside (outside) the nanoparticle, $E_0 = (\hbar k_0)^2/2m_{\text{in}}$, and Ψ_0 ($\Psi_{1\pm}$) is a wave function of the motion of the electron along axis z in the initial (final, after the absorption of a photon) state [16]. Such states are calculated by taking the effective potential $\tilde{V}(z, k_{\parallel}) = 0$ for $z < 0$ and

$$\tilde{V}(z, k_{\parallel}) = V(z) + (m_{\text{out}}^{-1} - m_{\text{in}}^{-1})(\hbar k_{\parallel})^2/2 \quad (7)$$

for $z \geq 0$. The second term in Eq. (7) appears due to the discontinuity in the electron effective mass in $z = 0$. In the metal-semiconductor interface $m_{\text{out}} < m_{\text{in}}$, so the second term in Eq. (7) increases the effective height of the barrier in $z = 0$. W/m and $\Psi_0' \Psi_{1\mp}'/m^2$ are continuous functions of z in $z = 0$ [16].

Derivation of Eqs. (1)–(7), the method of calculations, and some properties of wave functions Ψ_0 and $\Psi_{1\pm}$ are described in Appendix A.

Combining Eqs. (1) and (2) we obtain

$$\eta_{\text{SPE}} = \frac{2\pi\hbar}{\varepsilon_{\text{in}}'' a} \int_{k_z, k_{\parallel}} dj_{\text{SPE}}, \quad (8)$$

where the length

$$a = \int_{V_p} |\mathcal{E}_{\text{in}}|^2 dV_p / \int_{S_p} |\mathcal{E}_{\text{in}}^{(n)}|^2 dS_p, \quad (9)$$

and dj_{SPE} is determined by Eqs. (3)–(6). Integrations in Eq. (9) are by the volume V_p and by the surface S_p of the nanoparticle; \mathcal{E}_{in} is the amplitude of the external electric field inside the nanoparticle and $\mathcal{E}_{\text{in}}^{(n)}$ is the component of this field normal to the interface inside the nanoparticle. In general a depends on the external electric field. For small spherical nanoparticles with a uniform electric field inside, a is the nanoparticle radius.

III. VOLUME PHOTOEMISSION

We derive an expression for internal quantum efficiency of the volume photoemission η_{VPE} following [17]. In [17] the well-known so-called three step photoemission model [28,29] has been adopted to the case of nanoparticles, as shown here in Appendix B.

We suppose that an electron in VPE participates in three quantum-mechanically independent (incoherent) processes: the hot electron generation, the transport to the nanoparticle surface without collisions with the probability W_t , and the passage through the surface of the metal to the semiconductor

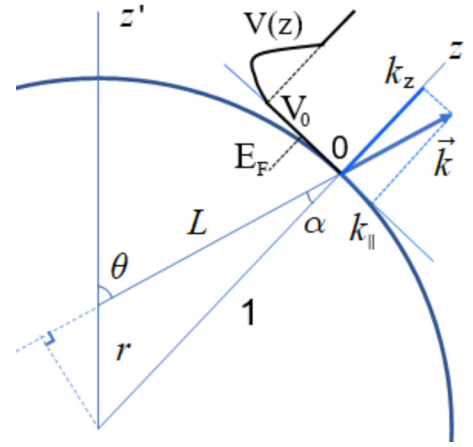


FIG. 2. Spherical coordinate system for calculations of η_{VPE} and components k_{\parallel} (k_z) of the electron wave vector \vec{k} parallel (perpendicular) to the nanoparticle-semiconductor interface shown by the blue semicircle. The potential barrier on the interface is shown by the black solid line.

environment with the probability W_p . The rate of generation of hot electrons in the unit of volume is r_{abs} defined in Eq. (1). The current of VPE, in electrons per second, is

$$J_{\text{VPE}} = \int_{V_p} r_{\text{abs}} \langle W_t W_p \rangle dV, \quad (10)$$

where

$$\langle W_t W_p \rangle = \frac{1}{n_h} \int W_t W_p f_h g d^3k$$

is averaged over hot electrons with the wave number k , distribution function f_h , and $g = 2/(2\pi)^3$;

$$n_h = \int f_h g d^3k, \quad d^3k = k^2 dk \sin\theta d\theta d\varphi$$

in the coordinate system shown in Fig. 2; n_h is the number of hot electron states in the unit of volume.

Parameters of hot electrons are the same everywhere in a small nanoparticle, therefore $W_p f_h g$ does not depend on spatial coordinates. So using the definition of η_{VPE} in Eq. (1) we write

$$\eta_{\text{VPE}} = n_h^{-1} \int \overline{W_t} W_p f_h g d^3k, \quad \overline{W_t} = V_p^{-1} \int W_t dV.$$

We take the probability that the hot electron is transported to the nanoparticle surface without collisions as in [17,30]:

$$W_t(r, \theta) = \exp[-L(r, \theta)/l_e], \quad (11)$$

where

$$L(r, \theta) = \sqrt{1 - r^2 \sin^2 \theta} - r \cos \theta$$

is the length of the path of the hot electron to the surface; l_e is the mean free path of the hot electron in the metal; L , r , and l_e are normalized to the radius a of the spherical nanoparticle (see Fig. 2). Following [25,31] we assume homogeneous distribution of hot electrons by the energies from E_F to $E_F + \hbar\omega$.

After transformations carried out in Appendix B we obtain

$$\eta_{\text{VPE}} = \frac{9l_e[1 - \exp(-2/l_e)]}{8(x_h^{3/2} - x_F^{3/2})} \times \int_1^{x_h} \sqrt{x} dx \int_0^{(1-1/x)/r_m} W_p(x, y) dy, \quad (12)$$

where $x_h = (E_F + \hbar\omega)/V_0$, $x_F = E_F/V_0$, $x = E/V_0$; $E = (\hbar k)^2/2m_{\text{in}}$ is the energy of the hot electron in metal and $y = r^2 \sin^2 \theta$ (see r and θ in Fig. 2). Only hot photoelectrons with real wave-vector component

$$\tilde{k}_z = \sqrt{[k^2(1 - r_m r^2 \sin^2 \theta) - k_V^2]}/r_m, \quad (13)$$

normal to the interface outside the nanoparticle, have enough energy to pass the barrier on the interface.

Formulas (8) and (12) determine η_{SPE} and η_{VPE} taking into account discontinuities in the electron effective mass, dielectric function, and potential barrier on the metal-semiconductor interface. They contain unknown $\Psi_{0, \pm}$ and W_p , which must be found for each specific potential barrier as described in Appendices A and D.

IV. COMPARISON OF EFFICIENCIES OF SURFACE AND VOLUME PHOTOEMISSIONS

We compare the efficiencies of the surface and the volume photoemissions in some examples. In these examples we neglect the thermal excitation of electrons, set $T = 0$ in Fermi distributions, and consider small spherical nanoparticles with the uniform electric field inside [32]. We suppose the step potential barrier

$$V = 0, \quad z < 0; \quad V = V_0, \quad z > 0,$$

so the second term $\approx V'(z) \equiv (dV/dz)_{z>0}$ in Eq. (5) is zero. We take well-known wave functions $\Psi_{0, \pm}$ for the step potential barrier as in [16]. In Appendix C we calculate $c_+^{(0)}$ and dj_{SPE} and find η_{SPE} , given by Eq. (C6).

In order to calculate η_{VPE} we find, in Appendix D, the probability $W_p(x, y)$, given by Eq. (D4), that the hot electron passes the step potential barrier with the discontinuity in the electron effective mass on the barrier. We insert Eq. (D4) into Eq. (12) and find η_{VPE} .

General expressions for $\eta_{\text{SPE, VPE}}$ are cumbersome, and we postpone their analysis for the future; here we consider in more detail a photoeffect near the red limit, i.e., with small excess of the photoelectron energy above the barrier:

$$\delta x_\omega \equiv (\hbar\omega + E_F)/V_0 - 1 \ll 1.$$

In this case only the electrons with $(\hbar k_z)^2/2m_{\text{in}} \approx E_F$ and $(\hbar k_{\parallel})^2/2m_{\text{in}} \approx 0$ contribute to SPE, as shown in Fig. 7. η_{SPE} for the step potential barrier is given by Eq. (C6) of Appendix C. We carry out the integration in Eq. (C6) near the red limit and find

$$\eta_{\text{SPE}} = \frac{a_S}{a} F_{em} \frac{\delta x_\omega^{5/2}}{\sqrt{r_m}}, \quad (14)$$

$$F_{em} = \frac{[1 + x_F + r_\varepsilon r_m(1 - x_F)]^2/4 + (r_\varepsilon - 1)^2 r_m(1 - x_F)}{x_F + r_m(1 - x_F)},$$

where a is the radius of the spherical nanoparticle. The length

$$a_S = \frac{4\lambda_{rb}}{15(2\pi)^2 \varepsilon_{rb}''} \frac{e^2}{\hbar c} \frac{\sqrt{x_F}}{(1 - x_F)^3} \quad (15)$$

is of the order of the maximum radius a , when SPE is still important; the wavelengths of applied field λ_{rb} and ε_{rb}'' correspond to the red limit. $a_S = 9.6$ nm for the gold spherical nanoparticle in the semiconductor with parameters as in [17]: $V_0 = 6.31$ eV, $E_F = 5.51$ eV, $\varepsilon_{\text{out}} = 13$, and the dielectric function of gold [16]

$$\varepsilon_{\text{in}} = 12 - \frac{(\lambda/0.136)^2}{1 + i\lambda/55},$$

where λ is the wavelength of the applied field in mkm. In examples below we take the nanoparticle radius a close to $a_S \approx 10$ nm.

We take the probability (D4) that the hot electron passes through the barrier in VPE and find, in the limit $\delta x_\omega \ll 1$, the approximate expression for W_p near the red limit:

$$W_p \approx 4\sqrt{r_m} \sqrt{\delta x_\omega - r_m y}.$$

We integrate Eq. (12) with this W_p and find

$$\eta_{\text{VPE}} \approx \frac{6}{5} \frac{l_e[1 - \exp(-2/l_e)]}{1 - x_F^{3/2}} \times \frac{\delta x_\omega^{5/2}}{\sqrt{r_m}}. \quad (16)$$

We see that near the red limit both η_{SPE} and η_{VPE} are proportional to $\delta x_\omega^{5/2}$, which is the same result as in [17] obtained without discontinuity in the electron effective mass.

Dependence (16) $\eta_{\text{VPE}} \sim 1/\sqrt{r_m}$ is weaker than the result $\eta_{\text{VPE}} \sim 1/r_m$ of [9], because $R_{\text{eff}}(0)$ (in our notation W_p) in Eq. (26) of [9] does not depend on r_m . It was found in [9] that the change in the electron effective mass increases (for $r_m > 1$) the potential barrier height as a consequence of the momentum conservation law. We note, in addition, that the decrease of the effective mass accelerates electrons outside the nanoparticle and increases the photocurrent. This is why our $W_p \sim \sqrt{r_m}$ [see the derivation of Eq. (D4) for W_p in Appendix D]. The net effect of decrease of effective mass still reduces VPE, because the passage through the barrier is possible for a smaller number of electrons with large kinetic energy, proportional to the square of electron velocity, while the photoemission current is increased proportional to the first power of that velocity.

In the case of SPE, the momentum conservation law also leads to $\eta_{\text{SPE}} \sim 1/\sqrt{r_m}$ [see Eq. (14)]. However, the net dependence on $r_m = \sqrt{m_{\text{out}}/m_{\text{in}}}$ is different in η_{SPE} and η_{VPE} due to the factor $F_{em}(r_m, r_\varepsilon)$ in Eq. (14). This factor is a consequence of the fact that SPE and VPE are qualitatively different processes. The photoabsorption and transmission of an electron through the barrier are described by a common wave function and interfere with each other in the SPE process. In contrast, VPE involves three quantum-mechanically incoherent processes: the absorption and generation of the hot electron, the transport of the hot electron to the barrier, and the transmission of the electron through the barrier. These processes are not described by a common wave function and they do not interfere with each other quantum mechanically.

Figure 3 shows spectra $\eta_{\text{SPE}}(\omega)$ given by Eq. (C3) and $\eta_{\text{VPE}}(\omega)$ given by Eq. (12) with W_p given by Eq. (D4) and

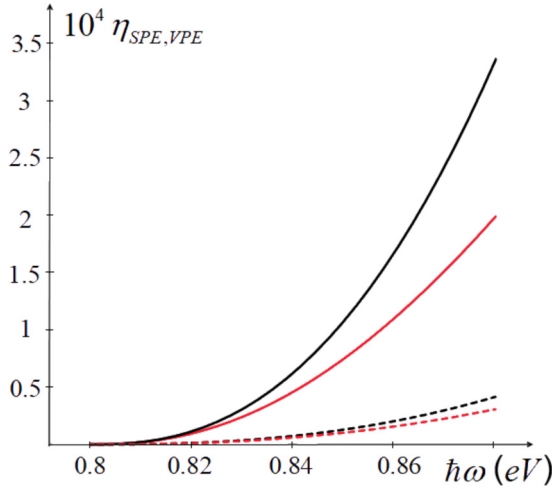


FIG. 3. Spectra of η_{SPE} (solid curves) and η_{VPE} (dashed curves) for the step potential barrier near the red limit of the photoeffect (black) and calculated exactly (red) by Eq. (C6) and by Eq. (12) for the gold spherical nanoparticle in the semiconductor.

their approximations near the red limit (14) and (16) for gold spherical nanoparticles of radius $a = 8.4$ nm in the semiconductor with $\epsilon_{\text{out}} = 13$, the electron mean free path (normalized to a) $l_e = 0.5$, and $r_m = 2$. We see from Fig. 3 that SPE (solid curves) is more efficient than VPE (dashed curves): $\eta_{\text{SPE}} > \eta_{\text{VPE}}$. We also see that the approximate calculation of $\eta_{\text{SPE,VPE}}$ near the red limit leads to good results, when the relative excess δx_ω of the photon energy above the red limit is less than 10–15%.

Figure 4 shows $\eta_{\text{SPE}}(\omega)$ given by Eqs. (1)–(6) and $\eta_{\text{VPE}}(\omega)$ given by Eq. (12) for $\epsilon_{\text{out}} = 13$ (the orange curve) and $\epsilon_{\text{out}} = 16$ (the red curve), $r_m = 2$, and the nanoparticle of diameter $2a = 15$ nm. $\eta_{\text{SPE}} > \eta_{\text{VPE}}$, if the photon energy is not too large. We see that SPE is more efficient than VPE, also for plasmon resonance frequencies marked by vertical dashed

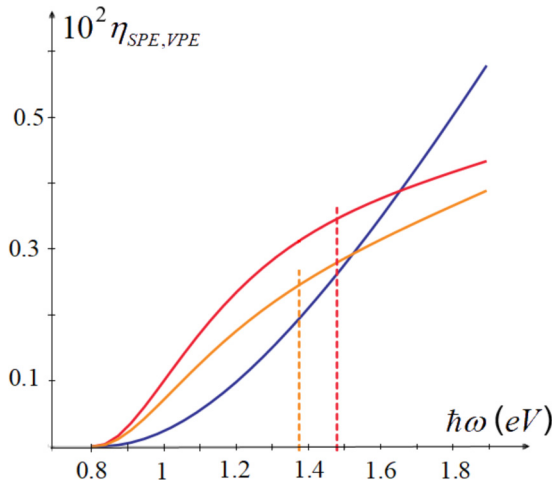


FIG. 4. Spectra of η_{VPE} (blue curve) and η_{SPE} (red and orange curves for $\epsilon_{\text{out}} = 13$ and $\epsilon_{\text{out}} = 16$) given by Eq. (12) and Eqs. (1)–(6) for the step potential barrier. Vertical dotted lines denote plasmon resonance frequencies. Diameter of spherical nanoparticle $2a = 15$ nm; other parameters are the same as for Fig. 3. $\eta_{\text{SPE}} > \eta_{\text{VPE}}$ (also at plasmon resonance frequencies) if $\hbar\omega$ is not too large.

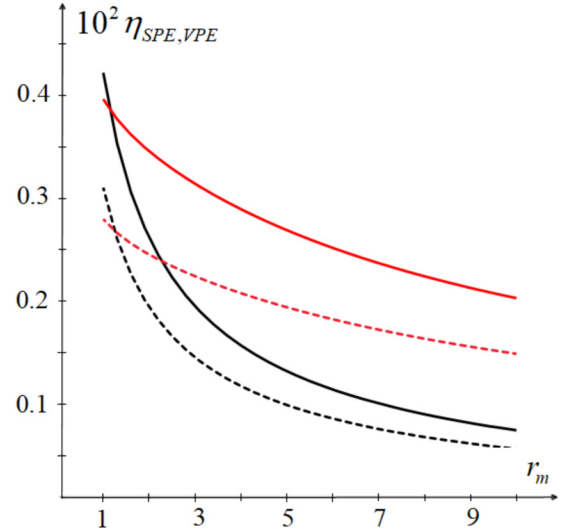


FIG. 5. η_{SPE} (red) and η_{VPE} (black) curves at plasmon resonance frequencies vs r_m characterizing the electron effective mass change. The semiconductor environment with $\epsilon_{\text{out}} = 13$ (16) corresponds to solid (dashed) curves. The difference in η_{VPE} (black curves) in different environments is because of the difference in the plasmon resonance frequencies. $\eta_{\text{SPE}} > \eta_{\text{VPE}}$ everywhere, apart from a small region near $r_m = 1$.

lines in Fig. 4. In the agreement with results of [17], η_{SPE} increases with the ratio $|\epsilon| = |\epsilon_{\text{in}}/\epsilon_{\text{out}}|$ between dielectric functions $\epsilon_{\text{in}} < 0$ in the metal and $\epsilon_{\text{out}} > 0$ in the semiconductor environment.

Figure 5 shows η_{SPE} and η_{VPE} as functions of $r_m = m_{\text{in}}/m_{\text{out}}$ for gold spherical nanoparticles in the semiconductor environment with $\epsilon_{\text{out}} = 13$ or 16 at plasmon resonance frequencies. Both η_{SPE} and η_{VPE} decrease with increase of r_m , but η_{SPE} (red curves) decreases with r_m more slowly than η_{VPE} (black curves). SPE is more efficient than VPE: $\eta_{\text{SPE}} > \eta_{\text{VPE}}$ (in the same environment) everywhere, apart from a small region near $r_m = 1$.

V. DISCUSSION

Both η_{SPE} and η_{VPE} are decreased with $r_m = m_{\text{in}}/m_{\text{out}}$ as a result of the momentum conservation law. We will explain why η_{SPE} decreases with r_m more slowly than η_{VPE} , as it is seen in Figs. 3–5.

A photoelectron passes the barrier and enters the semiconductor environment, if its wave-vector component perpendicular to the interface (\tilde{k}_{1z} for SPE and \tilde{k}_z for VPE) is real and positive. Demanding real \tilde{k}_{1z} in Eq. (4) and real \tilde{k}_z in Eq. (13) we find necessary conditions for SPE and VPE in terms of the angle α of incidence (see Fig. 2) of the electron on the metal-semiconductor interface:

$$\begin{aligned} \sin^2 \alpha &< \sin^2 \alpha_{\text{SPE}} = \delta x_\omega / (r_m x_0), \\ \sin^2 \alpha &< \sin^2 \alpha_{\text{VPE}} = \delta x_\omega / [r_m (x_0 + x_\omega)]. \end{aligned} \quad (17)$$

Here $\alpha_{\text{SPE,VPE}}$ are maximum angles of incidences of photoelectrons, able to pass the barrier, on the nanoparticle surface; $x_z = x_0 \cos^2 \alpha$ ($x_{\parallel} = x_0 \sin^2 \alpha$) is the normalized energy of the motion of the electron perpendicular (parallel) to the interface, and $x_0 = E_0/V_0$ is the normalized energy of an electron

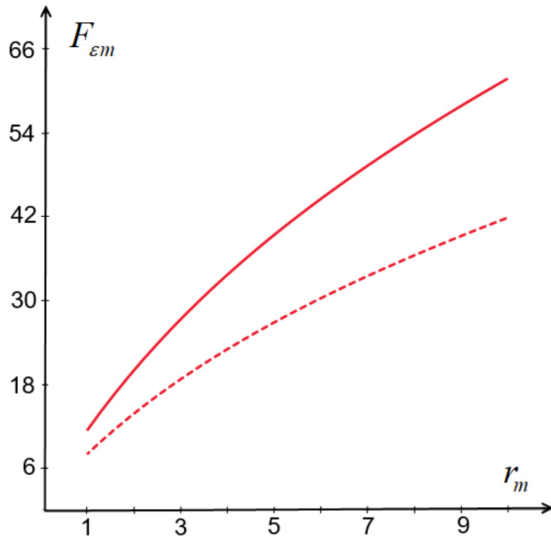


FIG. 6. Near the red limit $\eta_{\text{SPE}}(r_m)$ is different with $\eta_{\text{VPE}}(r_m)$ by factor $F_{\epsilon m}$; see Eqs. (14) and (16). The solid curve is for $\epsilon_{\text{in}} = 13$; the dashed curve is for $\epsilon_{\text{in}} = 16$.

before absorption. So electrons, available for photoemissions, fly inside cones with angles $\alpha_{\text{SPE,VPE}}$. The cone of electrons available for VPE has been found also in [9].

When r_m increases, both α_{SPE} and α_{VPE} decrease. However, α_{VPE} and the number of electrons available for VPE decrease with r_m faster than α_{SPE} , and this is why η_{SPE} is reduced with r_m more slowly than η_{VPE} . As a sign of this, factor $F_{\epsilon m}$, making the difference in $\eta_{\text{SPE}}(r_m)$ given by Eq. (14) and $\eta_{\text{VPE}}(r_m)$ given by Eq. (16), increases with r_m as shown in Fig. 6. This figure also shows that the difference between η_{SPE} and η_{VPE} for fixed r_m is greater for larger ratio $|r_\epsilon| = |\epsilon_{\text{in}}/\epsilon_{\text{out}}|$ of dielectric functions inside and outside the nanoparticle.

Physically, $\alpha_{\text{SPE}} > \alpha_{\text{VPE}}$ because the electron at SPE interacts only with the normal component of the electric field, and the energy of the absorbed photon comes only to the motion of electrons in the direction normal to the interface. Such motion is affected by the potential barrier; it does not obey the momentum conservation law and, therefore, it does not require additional energy for passing the barrier with the discontinuity of the electron effective mass. The electron wave-vector component k_{\parallel} , parallel to the interface and preserved in the photoemission, remains the same as before absorption and, therefore, it is relatively small.

In contrast, in the case of VPE the energy of absorbed photons is, on average, equally distributed over all directions of motion, so k_{\parallel} in VPE belongs to the electron *after* absorption and, therefore, it is greater than k_{\parallel} in SPE. In order to satisfy the momentum conservation law, the hot electron in VPE must have larger energy for passing through the interface, relative to the electron in SPE. A smaller number of electrons with larger energy, passing through the barrier, makes VPE less efficient than SPE at the discontinuity in the electron effective mass.

We present here a qualitative explanation of why SPE is less affected by the change in the electron effective mass than VPE. More detailed analysis of the collective influence of discontinuities in the electron effective mass, dielectric function, and potential barrier must take into account quantum interference, described by the factor $F_{\epsilon m}(r_m, r_\epsilon)$ in Eq. (14)

near the red limit, and by a more complicated factor in general. Optimization of quantum interference in the absorption, the electron transport, and the emission processes in SPE for finding the maximum of η_{SPE} must be a subject of special research.

VI. CONCLUSION

Decrease of the electron effective mass on the metal-semiconductor interface reduces the photoemission efficiency. By comparison of the SPE with the VPE we conclude that SPE is less sensitive to the decrease of the effective mass than VPE. Because of that, we found that SPE from small metal nanoparticles of a size less than 10–20 nm is several times more efficient than VPE. This is true also at plasmon resonance, when the resonant field inside nanoparticles is large and the photoemission rate is high.

Recent experimental and theoretical studies have discovered that the electron photoexcitation rates from Ag surfaces may be significantly enhanced for frequencies of electromagnetic field well above the plasmon resonance, namely, at multiples of the bulk plasmon resonance frequencies [33]. Analysis in our paper might be useful for comparison of SPE and VPE in the above resonances.

Low sensitivity of SPE to the electron effective mass decrease is an advantage of SPE relative to VPE in nanoparticles. It is added to other advantages of SPE, such as the increase of the photoabsorption rate due to the discontinuity in the dielectric function and the insensitivity of SPE to losses in the nanoparticle volume [16,17]. All these advantages encourage the use of SPE for highly efficient generation of hot electrons from nanoparticles. General formulas (1)–(12) for quantum efficiencies SPE and VPE, derived in this paper, are helpful for finding conditions for the maximum efficiencies of SPE and VPE from metal nanostructures.

ACKNOWLEDGMENTS

I.E.P., A.V.U., and N.V.N. acknowledge the Russian Science Foundation (Grant No. 20-19-00559) for support.

APPENDIX A: DERIVATION OF THE GENERAL FORMULA FOR INTERNAL QUANTUM EFFICIENCY OF SPE

1. General formulas for probability amplitude for single electron photoemission

We will follow the procedure of [20]. Assume that the electron with the variable mass $m(z)$ and the energy E moves in metal parallel to axis z , normal to the metal-semiconductor interface, towards the interface. It is easy to generalize this treatment in the case of arbitrary direction of motion of an electron.

The interface is described by potential $V(z)$, constant along the interface, as shown in Fig. 1. The wave function $\Psi e^{-iE/\hbar}t$ of the electron can be found from the stationary Schrödinger equation with Hamiltonian H :

$$E\Psi = H\Psi,$$

$$H = \hat{T} + V(z), \quad \hat{T} = -\frac{\hbar^2}{2} \frac{d}{dz} \left(\frac{1}{m} \frac{d}{dz} \right), \quad (\text{A1})$$

where \hat{T} is the kinetic energy operator of an electron with variable mass $m(z)$.

Suppose that solutions of Eq. (A1) are well known. We choose and normalize two linear independent solutions $\Psi_{\pm}(E)$ of Eq. (A1) such that $\Psi_{-} \rightarrow \exp(-ikz)$ at $z \rightarrow -\infty$ and $\Psi_{+} \rightarrow \exp(i\tilde{k}z)$ at $z \rightarrow \infty$, where k and \tilde{k} are wave numbers, correspondingly, at $z \rightarrow -\infty$ and ∞ . Thus, Ψ_{+} describes the electron propagating away from the interface in the semiconductor, i.e., at $z > 0$ far from the interface. Ψ_{-} describes a single electron propagating away from the interface in the metal, i.e., at $z < 0$. Ψ_{\pm} make a fundamental set of solutions of Eq. (A1).

We will describe the interaction of an electron with a classical electromagnetic field as a periodic perturbation $(1/2)\hat{U}e^{-i\omega t}$ of frequency ω . We neglect the emission of photons by the electron, so we preserve only the term $\approx e^{-i\omega t}$ in the perturbation and drop there the term $\approx e^{i\omega t}$.

Suppose the electron in the state Ψ_0 with the energy $E_0 < V_0$ collides with the interface, absorbs a photon from the electromagnetic field, and comes to the state Ψ_1 with the energy $E_1 = E_0 + \hbar\omega > V_0$, where V_0 is the energy of the bottom of the conduction band of the semiconductor environment (see Fig. 1). The wave function of the electron after the photoabsorption is

$$\Psi = \Psi_0 e^{-i(E_0/\hbar)t} + \psi e^{-i(E_1/\hbar)t}. \quad (\text{A2})$$

We insert the wave function (A2) into Schrödinger equation

$$i\hbar(\partial\Psi/\partial t) = [H + (1/2)\hat{U}e^{-i\omega t}]\Psi, \quad (\text{A3})$$

consider \hat{U} as a small perturbation, and neglect $\hat{U}\psi$. Then from Eq. (A3) we obtain the equation for ψ :

$$E_1\psi = H\psi + f(z), \quad f(z) = (1/2)\hat{U}\Psi_0. \quad (\text{A4})$$

According to [34], the solution ψ of the second-order linear inhomogeneous equation (A4) is expressed as a combination of fundamental solutions of corresponding homogeneous equation (A1). We denote fundamental solutions $\Psi_{\pm}(E_1)$ of Eq. (A1) as $\Psi_{1\pm}$ and write

$$\psi = C_{+}(z)\Psi_{1+} + C_{-}(z)\Psi_{1-}, \quad (\text{A5})$$

with

$$C_{\pm}(z) = \mp \frac{2}{\hbar^2} \int_{\mp\infty}^z dz' \frac{m(z')\Psi_{1\mp}(z')f(z')}{W(\Psi_{1-}\Psi_{1+})} + A_{\pm}, \quad (\text{A6})$$

where

$$W(\Psi_{1-}\Psi_{1+}) = \Psi_{1-}d\Psi_{1+}/dz - \Psi_{1+}d\Psi_{1-}/dz, \quad (\text{A7})$$

and A_{\pm} are constants determined from the boundary conditions. Expressions (A6) and (A7) follow from the standard mathematical approach [34].

In accordance with the asymptotic of $\Psi_{1+}(z)$ at $z \rightarrow \infty$, the first term in Eq. (A5) describes the electron moving away from the interface with the probability amplitude $C_{+}(\infty)$. We take $A_{+} = 0$, then $C_{+} \rightarrow 0$ at $z \rightarrow -\infty$, so the electron described by the first term in Eq. (A5) moves away from the metal, though it penetrates in the metal near the interface, where $C_{+}(z) \neq 0$. By setting $A_{-} = 0$ we see that $C_{-} \rightarrow 0$ at $z \rightarrow \infty$ and therefore the second term in Eq. (A5) describes the electron moving away from the interface in the

metal towards $z \rightarrow -\infty$, in accordance with the asymptotic of $\Psi_{1-}(-\infty)$.

We see that $C_{+}(\infty) \equiv C_{+}$ is a probability amplitude of photoemission of a single electron from the metal to the semiconductor. $C_{-}(-\infty)$ is a probability amplitude of generation of the hot electron in the metal due to the absorption of photons on the interface.

Taking into account that $\Psi_{1\pm}$ satisfy Eq. (A1) with $E = E_1$ we see that

$$\frac{d}{dz} \left(\frac{W}{m} \right) = -\frac{2}{\hbar^2} (\Psi_{1-}\hat{T}\Psi_{1+} - \Psi_{1+}\hat{T}\Psi_{1-}) = 0,$$

so $W(\Psi_{1-}\Psi_{1+})/m$ does not depend on z and can be taken out of the integral in Eq. (A6). Taking $z = \infty$ in Eq. (A6) we obtain the probability amplitude C_{+} of the photoemission of a single electron:

$$C_{+} = -\frac{m}{\hbar^2 W} \int_{-\infty}^{\infty} dz' \Psi_{1-}(z') \hat{U} \Psi_0(z'). \quad (\text{A8})$$

Photoemission probabilities are often formulated in terms of the so-called iLEED states [22] as the final photoelectron states; these states are the famous incoming wave solutions [23]. The probability amplitude C_{-} given by Eq. (A8) can be expressed in terms of iLEED states. For that we rewrite Eq. (A8) as

$$C_{+} = -(m/\hbar^2 W) \langle \Psi_{\text{iLEED}} | \hat{U} | \Psi_0 \rangle, \quad (\text{A9})$$

where $\langle \Psi_{\text{iLEED}} | \hat{U} | \Psi_0 \rangle$ denotes the matrix element of transition between the initial state $|\Psi_0\rangle = \Psi_0(z)$ and the final state $|\Psi_{\text{iLEED}}\rangle = \Psi_{1-}^*(z)$, where $\Psi_{1-}^*(z)$ is an iLEED state [22]. Indeed, $\Psi_{1-}(z)$ is a LEED state of an electron, which arrives from the semiconductor in $z = \infty$ to the interface, where the electron makes two scattered waves propagating away from the interface in both directions of axis z . In contrast, $\Psi_{1-}^*(z)$ has one emanation wave and two waves incident to the interface. An example of LEED state Ψ_{1-} is given by Eq. (C1) for the step potential barrier on the interface.

The state Ψ_{1+} is not an iLEED state. Ψ_{1+} contains one component approaching the interface and two components moving away from the interface, while iLEED state Ψ_{1-}^* contains two components directed to the interface and one component moving away [see Eq. (C1)]. However Ψ_{1+} can be chosen as a state of the photoemitted electron. Indeed, Ψ_{1+} describes an electron moving out of the interface in the semiconductor environment at $z \rightarrow \infty$; the probability $|C_{+}(\infty)|^2$ to find an electron in Ψ_{1+} in the semiconductor is not zero above the red photoemission limit. Otherwise, the probability $|C_{+}(-\infty)|^2$ to find an electron in the state Ψ_{1+} far from the interface in the metal is always zero, because of $C_{+}(-\infty) = 0$ in Eq. (A6) with $A_{+} = 0$.

An advantage of choosing Ψ_{1+} as a state of a photoemitted electron is that Ψ_{1+} appears in clear mathematical procedure of the perturbation theory, and that the probability amplitude $C_{+}(z \rightarrow \infty)$ of Ψ_{1+} coincides with the probability amplitude of the single electron photoemission at $z \rightarrow \infty$.

2. Probability amplitude with explicit \hat{U}

The integral in Eq. (A8), taken at $z = \pm\infty$, is the matrix element of \hat{U} for transition between Ψ_0 and $\Psi_{1\mp}^*$ states, as

explained in the final part of the previous subsection. Now we express this matrix element through the electromagnetic field and reduce the integral in Eq. (A8) to the form convenient for calculations.

We consider an electron moving along axis z normal to the interface. In order to describe the interaction of this electron with a classical electromagnetic field, we replace the momentum operator $\hat{p} = -i\hbar(d/dz)$ in Schrödinger equation (A1) by $\hat{p} - (e/c)\mathcal{A}$, where \mathcal{A} is the z component of the vector potential. We add $e\varphi$ to Eq. (A1), where e is the electron charge and φ is a scalar potential. Then, neglecting the term $\approx \mathcal{A}^2$ in $[\hat{p} - (e/c)\mathcal{A}]^2$, we find

$$\hat{U}\Psi_0 = \frac{i\hbar e}{2c} \left[\frac{d}{dz} \left(\frac{\mathcal{A}}{m} \Psi_0 \right) + \frac{\mathcal{A}}{m} \frac{d\Psi_0}{dz} \right] + e\varphi\Psi_0, \quad (\text{A10})$$

where c is the speed of light in vacuum. We insert (A10) into (A8). Integrating in Eq. (A8) by parts, removing terms coming to zero at $z = \pm\infty$, using $E_1 - E_0 = \hbar\omega$ and the fact that Ψ_0 satisfies Schrödinger equation (A1), and replacing φ by $\int_{-\infty}^z dz' (d\varphi/dz')$ and $-i\omega\mathcal{A}/c + d\varphi/dz$ by z component $\mathcal{E}^{(n)}$ of the electric field normal to the interface, we find after some transformations

$$C_{\pm}(\pm\infty) = -\frac{|e|m}{\hbar^2 W} \int_{-\infty}^{\infty} dz \Psi_0 \Psi_{1\mp} \int_{-\infty}^z \mathcal{E}^{(n)} dz'. \quad (\text{A11})$$

We see that the electron in SPE interacts only with the z component of the electromagnetic field normal to the interface.

Using that Ψ_0 and $\Psi_{1\pm}$ satisfy Schrödinger equation (A1) we represent $\Psi_0\Psi_{1\pm}$ as the derivative by z :

$$\frac{2\omega}{\hbar} \Psi_0 \Psi_{1\mp} = \frac{d}{dz} \left(\frac{W_{\pm}}{m} \right), \quad W_{\pm} = \Psi_{1\mp} \frac{d\Psi_0}{dz} - \Psi_0 \frac{d\Psi_{1\mp}}{dz}.$$

Then we integrate Eq. (A11) by parts, drop the terms coming to zero at $z \rightarrow \pm\infty$, and, after some transformations, obtain instead of Eq. (A11)

$$C_{\pm}(\pm\infty) = \frac{|e|m}{\hbar\omega W} \int_{-\infty}^{\infty} dz \left(E_m \frac{d\Psi_0}{dz} \Psi_{1\mp} + \frac{\Psi_{1\mp} \Psi_0}{2} \frac{dE_m}{dz} \right), \quad (\text{A12})$$

where we denote $E_m = \mathcal{E}^{(n)}/m$. Equation (A12) for the probability amplitude C_+ is Eq. (1) of [16] with W_1 denoted as W .

3. Discontinuities in the probability amplitude

It is convenient to extract in C_{\pm} the terms related to discontinuities in the surface potential $V(z)$, electromagnetic field $\mathcal{E}^{(n)}(z)$, and electron mass $m(z)$ in $z = 0$. We show how to do this through the example of when $\mathcal{E}^{(n)}$ and m are constants,

so that

$$C_{\pm}(\pm\infty) = \frac{|e|\mathcal{E}^{(n)}}{\hbar\omega W} \int_{-\infty}^{\infty} \frac{d\Psi_0}{dz} \Psi_{1\mp} dz. \quad (\text{A13})$$

We introduce operator $\hat{S} = H - E_0$. We see that $\hat{S}\Psi_0 = 0$ and $\hat{S}\Psi_{1\pm} = \hbar\omega\Psi_{1\pm}$. We insert $\Psi_{1\pm} = (\hbar\omega)^{-1}\hat{S}\Psi_{1\pm}$ into Eq. (A13) and obtain

$$C_{\pm}(\pm\infty) = \frac{|e|\mathcal{E}}{W(\hbar\omega)^2} \int_{-\infty}^{\infty} dz \frac{d\Psi_0}{dz} (\hat{S}\Psi_{1\mp}). \quad (\text{A14})$$

Operator \hat{S} (as well as H) is Hermitian, therefore

$$\int_{-\infty}^{\infty} dz \frac{d\Psi_0}{dz} (\hat{S}\Psi_{1\pm}) = \int_{-\infty}^{\infty} dz \Psi_{1\pm} \left(\hat{S} \frac{d\Psi_0}{dz} \right).$$

Because $\hat{S}\Psi_0 = 0$, and only $V(z)$ in \hat{S} depends on z , we write

$$0 = \frac{d}{dz} (\hat{S}\Psi_0) \equiv \hat{S} \frac{d\Psi_0}{dz} + \frac{dV(z)}{dz} \Psi_0$$

and therefore $\hat{S}(d\Psi_0/dz) = -[dV(z)/dz]\Psi_0$. Combining the last two expressions we obtain instead of Eq. (A14)

$$C_{\pm}(\pm\infty) = -\frac{|e|\mathcal{E}^{(n)}}{W(\hbar\omega)^2} \int_{-\infty}^{\infty} dz \frac{dV}{dz} \Psi_0 \Psi_{1\mp}.$$

Taking $dV(z)/dz = V_0\delta(z)|_{z=0} + V'(z)|_{z>0}$ with constant V_0 , delta function $\delta(z)$, and the differentiation by z denoted by a prime we write

$$C_{\pm} = -\frac{|e|\mathcal{E}^{(n)}}{W(\hbar\omega)^2} \left[V_0(\Psi_0\Psi_{1\mp})_{z=0} + \int_{+0}^{\infty} V'\Psi_0\Psi_{1\mp} dz \right].$$

Here the first term describes the discontinuity of potential $V(z)$ in $z = 0$ and the second term describes the influence of the continuous part of $V(z)$.

Using operator \hat{S} in a similar way, we treat the case of all $V(z)$, $\mathcal{E}^{(n)}(z)$, and $m(z)$ with discontinuities in $z = 0$ and obtain

$$C_+ = \frac{|e|m}{W(\hbar\omega)^2} \int_{-\infty}^{\infty} \frac{dz}{m} (c_V + c_{\mathcal{E}} + c_m), \quad (\text{A15})$$

which is Eq. (2) of [16] with

$$c_V = -\mathcal{E}^{(n)} V' \Psi_0 \Psi_{1-},$$

$$c_{\mathcal{E}} = \mathcal{E}^{(n)'} \left[\frac{\hbar^2}{2m} \Psi_0' \Psi_{1-}' + \left(E_0 - V + \frac{\hbar\omega}{2} \right) \Psi_0 \Psi_{1-} \right],$$

$$c_m = -\frac{\mathcal{E}^{(n)} m'}{m} \left(E_0 - V + \frac{\hbar\omega}{2} \right) \Psi_0 \Psi_{1-}. \quad (\text{A16})$$

Inserting (A16) into (A15) we find

$$C_+ = \frac{|e|m}{W(\hbar\omega)^2} \int_{-\infty}^{\infty} dz \left\{ -\left(\frac{\mathcal{E}^{(n)} V}{m} \right)' + \left(E_0 + \frac{\hbar\omega}{2} \right) \left(\frac{\mathcal{E}^{(n)}}{m} \right)' \right\} \Psi_0 \Psi_{1-} + \mathcal{E}^{(n)'} \frac{\hbar^2 \Psi_0' \Psi_{1-}'}{2m^2}. \quad (\text{A17})$$

Expression (A17) remains true for an arbitrary angle of incidence of the electron on the interface, if the surface potential V does not depend on x and y coordinates along the interface, so the electron wave function is factorized as in Eq. (A18). There $\Psi_i(z)$, where $i = \{0, 1\pm\}$, describe z

components of the motion of electrons perpendicular to the interface.

If $f(z)$ is a discontinuous function in $z = 0$ with $f(+0) = f_+$ and $f(-0) = f_-$, then $f'(z)_{z=0} = (f_{+0} - f_{-0})\delta(0)$. We consider a product of discontinuous functions as a

single discontinuous function. Therefore $(\mathcal{E}^{(n)}V/m)'_{z=0} = (\mathcal{E}_{\text{out}}^{(n)}V_0/m_{\text{out}})\delta(0)$, taking into account that $V(z < 0) = 0$; $(\mathcal{E}^{(n)}/m)'_{z=0} = (\mathcal{E}_{\text{out}}^{(n)}/m_{\text{out}} - \mathcal{E}_{\text{in}}^{(n)}/m_{\text{in}})\delta(0)$, where m_{in} (m_{out}) and $\mathcal{E}_{\text{in}}^{(n)}$ ($\mathcal{E}_{\text{out}}^{(n)}$) are amplitudes of the electron mass and normal component of the electric field inside (outside) the nanoparticle near its surface. From the boundary conditions for the field we find $\mathcal{E}_{\text{in}}^{(n)}/\mathcal{E}_{\text{out}}^{(n)} = \varepsilon_{\text{out}}/\varepsilon_{\text{in}}$, where ε_{in} (ε_{out}) is the dielectric function inside (outside) the nanoparticle.

After the integration in (A17) with delta functions we obtain

$$C_+ = c_+ \mathcal{E}_{\text{in}}^{(n)},$$

where c_+ is given by Eqs. (5) and (6) of the main text.

As general properties, one can see from Eqs. (5) and (6) that the value of the probability amplitude C_+ depends on the overlapping of Ψ_0 and Ψ_- , of Ψ'_0 and Ψ'_- in $z = 0$, and of $V'\Psi_0\Psi_-$ at $z > 0$. Conditions for the maximum overlapping at proper symmetry of $\Psi_0(z)$ and $\Psi_-(z)$ near $z = 0$ must be a subject of special research, taking into account the interference between different terms at calculations of $|C_+|^2$. In any case, in the model of $V(z)$ flat in directions parallel to the interface, an electron will interact only with the z component of the electromagnetic field normal to the interface.

4. Calculations of wave functions

We will discuss calculations of wave functions $\Psi_{0,1\pm}$ in Eqs. (5) and (6). For the electron moving along axis z perpendicular to the interface, $\Psi_{0,1\pm}$ are solutions of “unperturbed” (i.e., taken without the interaction with the electromagnetic field) Schrödinger equation (A1) with $E = E_{0,1}$ and potential $V(z) = 0$ for $z < 0$, $V(z = 0) = V_0$, and some continuous function $V(z)$ for $z > 0$ as shown in Fig. 1.

Ψ_0 corresponds to the electron before absorption of a photon, and $\Psi_{1\pm}$ corresponds to the electron after absorption of a photon. In the metal, after absorption, the electron has kinetic energy $E_1 = E_0 + \hbar\omega$, where $E_0 = (\hbar k_0)^2/2m_{\text{in}}$ is the initial energy of the electron with wave number k_0 in the metal before absorption. $\Psi_{1+}(z \rightarrow \infty) \rightarrow e^{i\tilde{k}_1 z}$ describes the electron with the wave number $\tilde{k}_1 = \sqrt{2m_{\text{out}}(E_1 - V_0)}/\hbar$ moving to the right in the conduction band of the semiconductor environment away from the interface (see Fig. 1).

$\Psi_{1-}(z \rightarrow -\infty) \rightarrow e^{-i\tilde{k}_1 z}$ corresponds to the electron with the wave number $k_1 = \sqrt{2m_{\text{in}}E_1}/\hbar$, reflected from the interface after absorption of a photon and moving to the left away from the interface in the metal.

Now we consider an electron moving at an arbitrary angle to the metal-semiconductor interface. We factorize the wave function of such an electron:

$$\Psi_i(z)e^{i\vec{k}_{\parallel}\vec{\rho}}, \quad (\text{A18})$$

where indices $i = \{0, 1+, 1-\}$ mark the same states of the electron as discussed before, $e^{i\vec{k}_{\parallel}\vec{\rho}}$ describes the motion of the electron parallel to the interface, $\vec{k}_{\parallel} = \{\vec{e}_x k_x, \vec{e}_y k_y\}$, $\vec{\rho} = \{\vec{e}_x x, \vec{e}_y y\}$, and \vec{e}_x and \vec{e}_y are unit vectors of the Cartesian coordinate system with axes x and y parallel to the interface shown in Fig. 2. Approximation (A18) has been used in [20,21] with the assumption that the potential barrier is averaged over x and y , so it is flat in these directions. In such a flat approximation

for $V(z)$, the medium dielectric function ε and the electron effective mass m do not depend on x and y , so \vec{k}_{\parallel} in Eq. (A18) is preserved and remains the same as in the initial state of the electron.

The wave function of the initial state of the electron before absorption is $\Psi_0(z) = e^{ik_z z}$, where $(\hbar k_z)^2/2m_{\text{in}} = E_z$ is a part of the electron kinetic energy related with the motion perpendicular to the interface, and k_z is the z component of the wave vector of the electron.

$\Psi_{1\pm}(z)$ are solutions of stationary Schrödinger equation (A1) with $E = E_z + \hbar\omega$ and $V(z)$ replaced by $\tilde{V}(z, k_{\parallel})$ given by Eq. (7).

It can be shown that only the component of the external electric field perpendicular to the interface interacts with an electron with an arbitrary angle of incidence on the interface.

APPENDIX B: GENERAL EXPRESSION FOR INTERNAL QUANTUM EFFICIENCY OF VPE

We consider the VPE for small spherical nanoparticles, following [17], in the three-step photoemission model [28,29] and suppose that an electron in VPE is involved in three quantum-mechanically incoherent processes: (i) the absorption of a photon, (ii) the passage to the interface without collision, and (iii) the transition through the interface. For simplicity, we suppose that only electrons absorb photons, and neglect other kinds of absorption as by impurities, etc. Then the rate of absorption r_{abs} , given in Eqs. (1) of the main text, is also the rate of generation of hot electrons in the unit of volume. The rate of photoemission of hot electrons from the unit of volume is, therefore,

$$r_{\text{VPE}} = r_{\text{abs}} W_t W_p, \quad (\text{B1})$$

where W_t is the probability that the hot electron avoids inelastic collisions and reaches the nanoparticle surface; W_p is the probability that the hot electron passes through the barrier on the surface and leaves the nanoparticle. Then the current of photoemission from the volume of the nanoparticle, in electrons per second, is

$$J_{\text{VPE}} = \int_{V_p} r_{\text{abs}} \langle W_t W_p \rangle dV, \quad (\text{B2})$$

where

$$\langle W_t W_p \rangle = \frac{1}{n_h} \int W_t W_p f_h g d^3 k$$

is averaged over hot electrons with the distribution function f_h , the density of states in the unit of volume $g = 2/(2\pi)^3$, $d^3 k = k^2 dk \sin \theta d\theta d\varphi$, and $n_h = \int f_h g d^3 k$ is the number of hot electron states in the unit of volume. θ and φ are polar and azimuthal angles in the spherical coordinate system with polar axes z' shown in Fig. 2.

The internal quantum efficiency of VPE is

$$\eta_{\text{VPE}} = J_{\text{VPE}}/R_{\text{abs}}, \quad (\text{B3})$$

where R_{abs} is the rate of absorption of photons in the nanoparticle given by Eq. (1) of the main text. We consider small spherical nanoparticles, with constant energy density $|E_{\text{in}}|^2$ of the electric field inside. Then, combining Eqs (B2) and (B3)

and R_{abs} from Eqs.(1) we write

$$\eta_{\text{VPE}} = \frac{1}{n_h V_p} \int W_t W_p f_h g d^3 k dV. \quad (\text{B4})$$

Parameters of hot electrons everywhere inside a small nanoparticle are the same, therefore $W_p f_h g$ in Eq. (B4) does not depend on spatial coordinates, so we simplify Eq. (B4) by separating their integrations:

$$\eta_{\text{VPE}} = \frac{1}{n_h} \int \bar{W}_t W_p f_h g d^3 k, \quad \bar{W}_t = \frac{1}{V_p} \int W_t dV. \quad (\text{B5})$$

Following [25,31] we approximate the distribution of hot electrons by homogeneous distribution over the energies from E_F to $E_F + \hbar\omega$ so $f_h = 1$ for $k_F^2 < k^2 < k_F^2 + k_\omega^2$ and $f_h = 0$ otherwise; $k_F = \sqrt{2m_{\text{in}}E_F/\hbar}$; $k_\omega = \sqrt{2m_{\text{in}}\omega/\hbar}$.

Nothing depends on angular coordinates in space and on azimuthal angle in k space in spherical nanoparticles, so the integration by these variables in Eq. (B4) gives 4π and 2π , respectively. We calculate

$$n_h = 4\pi \int_{k_F}^{k_h} \frac{2}{(2\pi)^3} k^2 dk = \frac{k_h^3 - k_F^3}{3\pi^2},$$

where $k_h^2 = k_F^2 + k_\omega^2$, use the spatial coordinate r normalized to the radius a of small spherical nanoparticles, and come from Eq. (B4) to

$$\eta_{\text{VPE}} = \frac{9}{2(k_h^3 - k_F^3)} \int_0^1 r^2 dr \int_{k_F}^{k_h} k^2 dk \times \int_0^\pi \sin\theta d\theta W_t(r, \theta) \text{Re}[W_p(k, \theta)]. \quad (\text{B6})$$

We take $\text{Re}[W_p(k, \theta)]$ in Eq. (B6); because we consider only hot electrons passing the barrier, such electrons fly inside the cone with $0 < \alpha < \alpha_{\text{VPE}}$ [9] (see α in Fig. 2); α_{VPE} is given by the second of Eqs. (17) of the main text. For such electrons $W_p(k, \theta)$ is real; otherwise $W_p(k, \theta)$ is purely imaginary. We rewrite Eq. (B6) in terms of dimensionless variables

$$x = E/V_0, \quad x_F = E_F/V_0, \quad x_h = (E_F + \hbar\omega)/V_0 \quad (\text{B7})$$

keeping, for simplicity, the same notations for $W_p(k, \theta)$ and $W_p(x, \theta)$:

$$\eta_{\text{VPE}} = \frac{9}{4(x_h^{3/2} - x_F^{3/2})} \int_0^1 r^2 dr \int_1^{x_h} \sqrt{x} dx \times \int_0^\pi W_t(r, \theta) \text{Re}[W_p(x, \theta)] \sin\theta d\theta. \quad (\text{B8})$$

Following [17] we suppose that the hot electron moves ballistically without elastic collisions, and it cannot be emitted if it loses energy in, at least, the single inelastic collision. According to [30], the probability that the hot electron reaches the nanoparticle boundary without collisions is

$$W_t(r, \theta) = \exp[-L(r, \theta)/l_e], \quad (\text{B9})$$

where $L(r, \theta) = \sqrt{1 - r^2 \sin^2 \theta} - r \cos \theta$ is the length of the path of the hot electron to the interface shown in Fig. 2, r is the distance from the nanoparticle center to the point of generation of the hot electron, l_e is the mean free path of an

electron in the metal, and r and l_e are normalized on the radius of a spherical nanoparticle.

We simplify Eq. (B8) and separate their integrals as in Eq. (B5). First, we separate the integration by $d\theta$ in Eq. (B8) in two parts: from zero to $\pi/2$ and from $\pi/2$ to π . Probability W_p that hot electron passes the barrier depends on the normalized kinetic energy x of the electron and on the part $x \sin^2 \alpha$ of this energy, corresponding to the motion parallel to the interface. Therefore $W_p = W_p(x, \sin^2 \alpha)$. We note that $\sin^2 \alpha = r^2 \sin^2 \theta$ (see Fig. 2) and introduce in Eq. (B8) new variable $y = r^2 \sin^2 \theta$ instead of θ , so $W_p = W_p(x, y)$. We come from θ to y in Eqs. (B8) and (B9) taking into account that $\sin\theta d\theta = dy/(2r\sqrt{r^2 - y})$, introduce $z = r^2$, separate integrations in η_{VPE} as in Eq. (B5), and obtain

$$\eta_{\text{VPE}} = \frac{9/4}{x_h^{3/2} - x_F^{3/2}} \int_1^{x_h} \sqrt{x} dx \int_0^{y_m(x)} \bar{W}_t W_p dy, \quad (\text{B10})$$

where

$$\bar{W}_t(y) = \frac{1}{4} \int_y^1 \frac{dz}{\sqrt{z-y}} W_t(z, y) \quad (\text{B11})$$

with

$$W_t = e^{-\sqrt{1-y}/l_e} [e^{-\sqrt{z-y}/l_e} + e^{\sqrt{z-y}/l_e}], \quad (\text{B12})$$

where W_t is given by Eq. (B9). The integral (B11) can be taken and we obtain

$$\bar{W}_t(y) = \frac{l_e}{2} \left[1 - \exp\left(-\frac{2\sqrt{1-y}}{l_e}\right) \right]. \quad (\text{B13})$$

Now we determine $y_m(x)$ in Eq. (B10). The energy of the hot electron in metal is $(\hbar k)^2/2m_{\text{in}}$. When the electron passes through the barrier, the component $k \sin \alpha$ of its wave vector is preserved, while the component k_z normal to the interface is not preserved. The z component \tilde{k}_z of the wave vector of the emitted electron moving far from the barrier in the semiconductor environment is found from the energy conservation law

$$\hbar^2(\tilde{k}_z^2 + k^2 \sin^2 \alpha)/2m_{\text{out}} + V_0 = (\hbar k)^2/2m_{\text{in}}. \quad (\text{B14})$$

Taking $\sin \alpha = r \sin \theta$ (see Fig. 2), we obtain from Eq. (B14) the expression (13) for \tilde{k}_z . \tilde{k}_z must be real, so only electrons with $k > k_V$ flying inside a cone with $\sin \theta < \sin \theta_{\text{VPE}}$ pass through the barrier. From Eq. (13) we obtain

$$r^2 \sin^2 \theta < r^2 \sin^2 \theta_{\text{VPE}} \equiv y_{\text{VPE}}(x) = (1 - 1/x)/r_m,$$

where $x = k^2/k_V^2$. We suppose $r_m > 1$, which is typical for the metal-semiconductor interface; then

$$0 < y_{\text{VPE}}(x) < 1.$$

With the result (B13) we obtain

$$\eta_{\text{VPE}} = \frac{9l_e}{8(x_h^{3/2} - x_F^{3/2})} \int_1^{x_h} \sqrt{x} dx \times \int_0^{(1-1/x)/r_m} \left[1 - \exp\left(-\frac{2\sqrt{1-y}}{l_e}\right) \right] W_p(x, y) dy. \quad (\text{B15})$$

Since we do not know l_e precisely, we can ignore y dependence in $\exp(-\sqrt{1-y}/l_e)$ in Eq. (B15) and obtain the result (12) of the main text.

Our approach for VPE is similar to the three step photoemission model of [29], where the VPE from macroscopic metal photocathodes has been studied following [28]. There are also some differences between [29] and our approach. In particular, for the probability that the hot electron reaches the boundary without collision, we use expression (11) from [30], appropriate for small spherical nanoparticles. Authors of [29] for the same probability use their formula (4), which is appropriate for the macroscopic photocathode.

Another difference is that [29] uses the so-called 0-1 model for the surface potential, where the probability that the hot electron goes outside the metal is 0 or 1, depending on whether the electron flies below or above the barrier. The same 0-1 model is used in many papers, for example, in [9]. In contrast, we take the probability W_p that the hot electron passes the barrier and calculate W_p explicitly for the step potential barrier. This is why our photocurrent spectrum near

the red limit is $\approx \delta x_\omega^{5/2}$ [see Eq. (16)], not $\approx \delta x_\omega^2$ as in Eq. (12) of [29] and in [31].

We consider internal quantum efficiency of VPE, so we do not need the optical transmission coefficient $1 - R(\omega)$ in our η_{VPE} , as it is in [29]. There is no discontinuity in the electron effective mass on the metal-vacuum interface in [29].

The density of states available for hot electrons at zero temperature is the same in our case and in [29], though we integrate by hot electron states, but not by the initial states of electrons as in [29].

APPENDIX C: EXTERNAL QUANTUM EFFICIENCY OF SPE THROUGH THE STEP POTENTIAL BARRIER

Multipliers Ψ_0 and $\Psi_{1\pm}$ in wave functions (A18) describe the motion of an electron along axis z . For the step potential barriers, $V = 0$ for $z < 0$ and $V = V_0$ for $z > 0$, they are solutions of Schrodinger equation (A1) with E equal to $E_0 = (\hbar k_z)^2/2m_{\text{in}}$ for Ψ_0 and to $E_1 = E_0 + \hbar\omega$ for $\Psi_{1\pm}$ and $V(z \geq 0)$ given by Eq. (7) with $V(z) = V_0$. Such wave functions are

$$\begin{aligned}\Psi_0(z) &= [\exp(ik_z z) + A_0 \exp(-ik_z z)]_{z < 0} + B_0 \exp(-\tilde{k}_z z)_{z > 0}, \\ \Psi_{1+}(z) &= [A_{1+} \exp(ik_{1z} z) + B_{1+} \exp(-ik_{1z} z)]_{z < 0} + \exp(i\tilde{k}_{1z} z)_{z > 0}, \\ \Psi_{1-}(z) &= [A_{1-} \exp(i\tilde{k}_{1z} z) + B_{1-} \exp(-i\tilde{k}_{1z} z)]_{z > 0} + \exp(-ik_{1z} z)_{z < 0}\end{aligned}\quad (\text{C1})$$

where $\tilde{k}_z = \sqrt{[k_V^2 + k_{\parallel}^2(r_m - 1) - k_z^2]/r_m}$ is real, $k_{1z} = \sqrt{k_z^2 + k_\omega^2}$, $\tilde{k}_{1z} = \sqrt{[k_z^2 + k_\omega^2 - k_V^2 - k_{\parallel}^2(r_m - 1)]/r_m}$, $r_m = m_{\text{in}}/m_{\text{out}}$, $k_V = \sqrt{2m_{\text{in}}V_0/\hbar}$,

$$\begin{aligned}A_0 &= (1 - i\theta_0)/(1 + i\theta_0), & B_0 &= 2/(1 + i\theta_0), \\ A_{1-} &= (1 + \theta_1)/2, & B_{1-} &= (1 - \theta_1)/2, \\ A_{1+} &= (\theta_1 - 1)/2\theta_1, & B_{1+} &= (1 + \theta_1)/2\theta_1\end{aligned}$$

and

$$\begin{aligned}\theta_0 &= \sqrt{r_m[V(0)/E_0 - 1]}, \\ \theta_1 &= \sqrt{r_m[1 - V(0)/(E_0 + \hbar\omega)].}\end{aligned}$$

Using wave functions (C1) we obtain $\Psi_0\Psi_{1-}$, $\Psi_0'\Psi_{1-}'/m^2$, and W/m ; insert them into Eq. (6) of the main text; drop in Eq. (5) the second term $\approx V' \equiv dV/dz$; introduce dimensionless variables

$$x_z = (k_z/k_V)^2, \quad x_{\parallel} = (k_{\parallel}/k_V)^2, \quad x_\omega = (k_\omega/k_V)^2; \quad (\text{C2})$$

and find from Eq. (1) of the main text

$$\eta_{\text{SPE}} = \frac{a_s \sqrt{r_m}}{a} \int_0^\infty dx_{\parallel} \int_0^\infty \frac{dx_z}{\sqrt{x_z}} \text{Re} [\sqrt{x_z + x_\omega - 1 - x_{\parallel}(r_m - 1)}] |uK_{\text{dis}}|^2 f_F(x) [1 - f_F(x + x_\omega)], \quad (\text{C3})$$

where $f_F(x) = \{1 + \exp[(x - x_F)/x_T]\}^{-1}$ is Fermi-distribution function, which depends on the normalized kinetic energy of an electron $x = x_z + x_{\parallel}$; $x_F = E_F/V_0$, $x_T = K_B T/V_0$,

$$u = \frac{\sqrt{x_z}}{\{\sqrt{x_z} + i\sqrt{r_m[1 + x_{\parallel}(r_m - 1) - x_z]}\} \{\sqrt{x_z + x_\omega} + \sqrt{r_m[x_z + x_\omega - 1 - x_{\parallel}(r_m - 1)]}\}}, \quad (\text{C4})$$

$$K_{\text{dis}} = (r_\varepsilon r_m - 1) \left(x_z + \frac{x_\omega}{2}\right) - r_\varepsilon r_m [1 + x_{\parallel}(r_m - 1)] + i(r_\varepsilon - 1) \sqrt{r_m(x_z + x_\omega)} [1 + x_{\parallel}(r_m - 1) - x_z]. \quad (\text{C5})$$

Taking $r_m = 1$ we obtain $K_{\text{dis}} = -K_{\Delta\varepsilon}$, where $K_{\Delta\varepsilon}$ is given by Eq. (17) of [17] and $|u(x_z)|^2$ is the same as $G(x_z)$ given by Eq. (16) of [17]. We neglect the temperature dependence of the Fermi distribution $f_F(x)$, taking $f_F(x) = 1$ for $0 < x < x_f$ and $f_F(x) = 0$ otherwise, and obtain

$$\eta_{\text{SPE}} = \frac{a_0 \sqrt{r_m}}{a} \left(\int_{1-x_\omega}^{x_0} dx_z \int_0^{x_{\parallel 0}(x_z)} dx_{\parallel} + \int_{x_0}^{x_f} dx_z \int_0^{x_f - x_z} dx_{\parallel} \right) \frac{|uK_{\text{dis}}|^2}{\sqrt{x_z}} \text{Re} \sqrt{x_z + x_\omega - 1 - x_{\parallel}(r_m - 1)}. \quad (\text{C6})$$

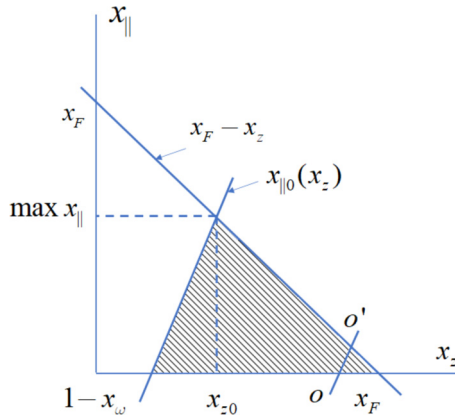


FIG. 7. The area of integration in Eq. (C6) is shadowed, $\max x_{\parallel} = (x_F + x_{\omega} - 1)/r_m$. The line oo' restricts the integration area for small excess of photon energy $x_{\omega} + x_F - 1 \ll x_F$ near the red limit of photoeffect, where $x_z \approx x_F$ and $x_{\parallel} \approx 0$.

Integration limits $x_{z0} = x_F + (1 - x_{\omega} - x_F)/r_m$ and $x_{\parallel 0} = (x_z + x_{\omega} - 1)/(r_m - 1)$ are shown in Fig. 7,

$$a_0 = \frac{\lambda_{rb}}{(2\pi)^2 \varepsilon''(x_{\omega}) \hbar c} \frac{e^2}{x_{\omega}^4} \frac{1 - x_F}{x_{\omega}^4}, \quad (\text{C7})$$

λ_{rb} is the wavelength of the external field on the red limit of the photoeffect, and ε'' is the imaginary part of the dielectric function of the metal of the nanoparticle.

APPENDIX D: THE STEP POTENTIAL BARRIER WITH DISCONTINUOUS IN THE ELECTRON EFFECTIVE MASS

We calculate the wave function of the hot electron in the coordinate system with axis z , normal to the nanoparticle sur-

face, shown in Fig. 2. Similar to the wave functions (A18) in SPE, the wave function of the hot electron in VPE is factorized as $\Psi_z(z)e^{i\tilde{k}_{\parallel}\tilde{\rho}}$. In Fig. 2 we see that

$$k_{\parallel} = k \sin \alpha, \quad k_z = k \cos \alpha \quad (\text{D1})$$

are components of the wave vector of the hot electron, parallel and perpendicular to the interface; the wave number of the hot electron is k . The z -dependent part of the wave function of the hot electron is

$$\Psi_z(z) = (e^{i\tilde{k}_z z} + A e^{-i\tilde{k}_z z})_{z < 0} + (B e^{i\tilde{k}_z z})_{z > 0}, \quad (\text{D2})$$

where A and B are c -number constants. The z component \tilde{k}_z of the wave vector of the hot electron for $z > 0$ is given by Eq. (13). Inserting the wave function (D2) into the boundary conditions on the interface in $z = 0$ $\Psi_h(-0) = \Psi_h(+0)$ and $m_{\text{in}}^{-1}(d\Psi_h/dz)_{z=0} = m_{\text{out}}^{-1}(d\Psi_h/dz)_{z=+0}$ we obtain $B = 2/(1 + r_m \tilde{k}_z/k_z)$. With the wave function (D2) the current of electrons in the z direction toward [away from] the interface is $j_z^{(\text{in})} = \hbar \tilde{k}_z/m_{\text{in}} [j_z^{(\text{out})} = (\hbar \tilde{k}_z/m_{\text{out}})|B|^2]$, so the probability that the hot electron passes through the barrier is

$$W_p(k, k_z) \equiv j_z^{(\text{out})}/j_z^{(\text{in})} = \frac{4r_m k_z \text{Re}(\tilde{k}_z)}{(k_z + r_m \tilde{k}_z)^2}, \quad (\text{D3})$$

if \tilde{k}_z is real, and $W_p = 0$ otherwise. Using dimensionless variables (B7) and $y = r^2 \sin^2 \theta$ we rewrite Eq. (D3) as

$$W_p(x, y) = \frac{4\sqrt{r_m x(1-y)[x(1-r_m y) - 1]}}{\{\sqrt{x(1-y)} + \sqrt{r_m[x(1-r_m y) - 1]}\}^2}. \quad (\text{D4})$$

- [1] H. Chalabi and M. L. Brongersma, Harvest season for hot electrons, *Nat. Nanotechnol.* **8**, 229 (2013).
- [2] M. Brongersma, N. Halas, and P. Nordlander, Plasmon-induced hot carrier science and technology, *Nat. Nanotechnol.* **10**, 25 (2015).
- [3] I. Goykhman, B. Desiatov, J. Khurgin, J. Shappir, and U. Levy, Locally oxidized silicon surface-plasmon Schottky detector for telecom regime, *Nano Lett.* **11**, 2219 (2011).
- [4] M. W. Knight, H. Sobhani, P. Nordlander, and N. J. Halas, Photodetection with active optical antennas, *Science* **332**, 702 (2011).
- [5] P. Berini, Surface plasmon photodetectors and their applications, *Laser Photonics Rev.* **8**, 197 (2014).
- [6] Y. Zhang, S. He, W. Guo, Y. Hu, J. Huang, J. R. Mulcahy, and W. D. Wei, Surface-plasmon-driven hot electron photochemistry, *Chem. Rev.* **118**, 2927 (2018).
- [7] M. Graf, D. Jalas, J. Weissmeijler, A. Y. Petrov, and M. Eich, Surface-to-volume ratio drives photoelectron injection from nanoscale gold into electrolyte, *ACS Catalysis* **9**, 3366 (2019).
- [8] C. Scales and P. Berini, Thin-film Schottky barrier photodetector models, *IEEE J. Quantum Electron.* **46**, 633 (2010).
- [9] J. B. Khurgin, Fundamental limits of hot carrier injection from metal in nanoplasmonics, *Nanophotonics* **9**, 453 (2020).
- [10] B. L. Rickman, J. A. Berger, A. W. Nicholls, and W. A. Schroeder, Intrinsic Electron Beam Emittance from Metal Photocathodes: The Effect of the Electron Effective Mass, *Phys. Rev. Lett.* **111**, 237401 (2013).
- [11] S. Karkare and I. Bazarov, Effect of nanoscale surface roughness on transverse energy spread from GaAs photocathodes, *Appl. Phys. Lett.* **98**, 094104 (2011).
- [12] N. Goncharuk, The influence of an emitter accumulation layer on field emission from a multilayer cathode, *Mater. Sci. Eng. A* **353**, 36 (2003).
- [13] S. Christov, Recent test and new applications of the unified theory of electron emission, *Surf. Sci.* **70**, 32 (1978).
- [14] R. Stratton, Theory of field emission from semiconductors, *Phys. Rev.* **125**, 67 (1962).
- [15] C. Crowell, Richardson constant and tunneling effective mass for thermionic and thermionic-field emission in Schottky barrier diodes, *Solid-State Electron.* **12**, 55 (1969).
- [16] I. E. Protsenko and A. V. Uskov, Photoemission from metal nanoparticles, *Phys. Usp.* **55**, 508 (2012).
- [17] A. V. Uskov, I. E. Protsenko, R. S. Ikhsanov, V. E. Babicheva, S. V. Zhukovsky, A. V. Lavrinenko, E. P. O'Reilly, and H. Xu, Internal photoemission from plasmonic nanoparticles:

- Comparison between surface and volume photoelectric effects, *Nanoscale* **6**, 4716 (2014).
- [18] S. Tan, Y. Dai, S. Zhang, L. Liu, J. Zhao, and H. Petek, Coherent Electron Transfer at the Ag/graphite Heterojunction Interface, *Phys. Rev. Lett.* **120**, 126801 (2018).
- [19] I. Tamm and S. Schubin, Zur theorie des photoeffektes an metallen, *Z. Phys.* **68**, 97 (1931).
- [20] A. Brodsky and Y. Gurevich, *Teoriya Elektronnoi Emissii iz Metallov (Theory of Electron Emission from Metals)* (Nauka, Moscow, 1973).
- [21] A. M. Brodskii and Yu. Ya. Gurevich, Theory of external photoeffect from the surface of a metal, *Sov. Phys. JETP* **27**, 114 (1968).
- [22] I. Adawi, Theory of the surface photoelectric effect for one and two photons, *Phys. Rev.* **134**, A788 (1964).
- [23] G. Breit and H. A. Bethe, Ingoing waves in final state of scattering problems, *Phys. Rev.* **93**, 888 (1954).
- [24] J. Pendry, Theory of photoemission, *Surf. Sci.* **57**, 679 (1976).
- [25] A. Novitsky, A. V. Uskov, C. Gritti, I. E. Protsenko, B. E. Kardynal, and A. V. Lavrinenko, Photon absorption and photocurrent in solar cells below semiconductor bandgap due to electron photoemission from plasmonic nanoantennas, *Progress in Photovoltaics: Research and Applications* **22**, 422 (2014).
- [26] A. V. Uskov, I. E. Protsenko, N. A. Mortensen, and E. P. O'Reilly, Broadening of plasmonic resonance due to electron collisions with nanoparticle boundary: A quantum mechanical consideration, *Plasmonics* **9**, 185 (2014).
- [27] S. V. Zhukovsky, V. E. Babicheva, A. V. Uskov, I. E. Protsenko, and A. V. Lavrinenko, Enhanced electron photoemission by collective lattice resonances in plasmonic nanoparticle-array photodetectors and solar cells, *Plasmonics* **9**, 283 (2014).
- [28] C. N. Berglund and W. E. Spicer, Photoemission studies of copper and silver: Theory, *Phys. Rev.* **136**, A1030 (1964).
- [29] D. H. Dowell and J. F. Schmerge, Quantum efficiency and thermal emittance of metal photocathodes, *Phys. Rev. ST Accel. Beams* **12**, 074201 (2009).
- [30] Q. Y. Chen and C. W. Bates, Geometrical Factors in Enhanced Photoyield from Small Metal Particles, *Phys. Rev. Lett.* **57**, 2737 (1986).
- [31] R. H. Fowler, The analysis of photoelectric sensitivity curves for clean metals at various temperatures, *Phys. Rev.* **38**, 45 (1931).
- [32] S. A. Maier, *Plasmonics: Fundamentals and Applications* (Springer, New York, 2007).
- [33] D. Novko, V. Despoja, M. Reutzel, A. Li, H. Petek, and B. Gumhalter, Plasmonically assisted channels of photoemission from metals, *Phys. Rev. B* **103**, 205401 (2021).
- [34] G. A. Korn and T. M. Korn, *Mathematical Handbook for Scientists and Engineers* (McGraw-Hill, New York, 1968).